COSMIC RAY ISOTOPE MEASUREMENTS WITH A NEW CERENKOV X TOTAL ENERGY TELESCOPE

W. R. Webber, J. C. Kish & D. A. Schrier
Space Science Center
University of New Hampshire
Durham, NH 03824

1. Introduction and Experimental Data. In this paper we report measurements of the isotopic composition of cosmic ray nuclei with Z = 7-20. These measurements were made with a new version of a Cerenkov x total E telescope. This telescope and the details of the balloon flight are described in paper OG 4.1-5. Path length and uniformity corrections are made to all counters to a RMS level < 1%. Since the Cerenkov counter is crucial to mass measurements using the C x E technique - special care was taken to optimize the resolution of the 2.4 cm thick Pilot 425 Cerenkov counter. This counter exhibited a β = 1 muon equivalent LED resolution of 24%, corresponding to a total of 90 p.e. collected at the 1st dynodes of the photomultiplier tubes.

Events to be analyzed using the C x E mass analysis technique are first selected according to charge by a two dimensional method using both dE/dx xE and dE/dx xC matrices. Three separate dE/dx measurements are utilized. Charge overlap is neglible. Mass histograms are constructed from C x E matrices for each charge as illustrated in Figure 1 for Oxygen nuclei. Mass histograms for N, O, Ne and Mg nuclei are shown in Figure 2, and for Al, Si, S, Ar and Ca nuclei in Figure 3. The mass resolution is $\sigma \sim 0.23$ AMU for ^{16}O and 0.27 AMU for ^{28}Si.

The data from the 30 hour balloon flight is summarized in Table I. Column 1 gives the energy interval for mass analysis. The upper limit is taken to be $C/C_{max} = 0.45$ for Mg and heavier nuclei. Column 2 gives the number of events observed. Errors are shown only for isotopes where significant mass overlap occurs - all other errors are taken to be statistical. Column 3 shows the charge fraction for each isotope corrected to equal energy/nucleon intervals. And finally Column 4 shows this charge fraction corrected to the top of the atmosphere.

2. Interpretation of the Data. The basic goal of this experiment is to compare the observed isotopic ratios with those expected after interstellar propagation in order to derive the cosmic ray source abundance ratios. The secondary abundances produced during propagation are calculated using new cross sections measured by our group at the BEVALAC (Webber et al., paper OG 7.2-2). The propagation program utilizes a simple exponential path length distribution in hydrogen with a mean path length $\lambda_e = 23.0\ \beta\ P^{-0.6}\ g/cm^2$ above 5.5GV and $\lambda_e = 8.33\ \beta$ below 5.5GV. The solar modulation parameter Φ = 600 MV. At an interstellar energy ~ 800 MeV/nuc appropriate to these measurements, $\lambda_e \sim 6.8 g/cm^2$.

The extrapolation to the source for selected isotope ratios is shown in Table II. Also shown for comparison are previously measured isotope ratios (at a slightly lower energy) from a summary by Wiedenbeck, 1984. These differ slightly from the original values quoted by Wiedenbeck and co-workers from the ISEE experiment.

Below is a charge by charge summary of our results.
Nitrogen. Nitrogen above the Cerenkov threshold stops near the end of the 2nd and

last total E counter in our telescope. The resulting energy range of analysis is narrow, thus limiting the statistical accuracy of the data. The results obtained here are consistent with earlier results showing a significantly greater abundance of ^{15}N than ^{14}N at earth.

Oxygen. The ^{17}O and ^{18}O abundances that we observe are slightly larger than, but consistent with those originally reported by Wiedenbeck and Greiner, 1981a. It is seen that the secondary production of ^{18}O is ~ 10 x the solar system abundance ratio making it very difficult to achieve a meaningful source abundance determination of this isotope.

Neon. The relative abundances for ^{21}Ne and ^{22}Ne we measure are in good agreement with those reported by Wiedenbeck and Greiner, 1981a. ^{21}Ne is consistent with being all secondary and the source abundance ratio $^{22}Ne/^{20}Ne$ that we derive is ~ 4 x the solar system value in agreement with earlier measurements.

Magnesium. The relative abundances of ^{25}Mg and ^{24}Mg we measure are again consistent with, but slightly smaller than those originally reported by Wiedenbeck and Greiner, 1981a. (They agree even better with the average abundance ratios summarized by Wiedenbeck, 1984 - see Table II) These slightly lower abundance fractions - coupled with a secondary production which appears to be 20 - 40% larger than that used by the above authors leads to cosmic ray source abundances of these nuclei that are 1.43 ± 0.50 x the solar system ratio for $^{25}Mg/^{24}Mg$, and 1.24 ± 0.28 x the solar system ratio for $^{26}Mg/^{24}Mg$. These values are lower than those originally reported by the above authors, but are in agreement within the quoted ± 1 σ experimental errors. They are also consistent with cosmic ray source to solar system ratios of one.

Aluminum. The fraction $^{26}Al/^{27}Al$ of 2.2 ± 1.8% that we measure compares with the fraction of 3.6 ± 2.9% reported by Wiedenbeck, 1983.

Silicon. The fractions we measure for ^{29}Si and ^{30}Si are about 1 σ lower than those originally reported by Wiedenbeck and Greiner, 1981b. For the secondary production of these isotopes we obtain ~ 30-40% more than appears to have been obtained by the above authors. This leads to cosmic ray source fractions of these isotopes which are 0.79 ± 0.42 and 0.82 ± 0.58 x the solar system values respectively. These values are ~ 2 σ below the original values quoted by the above authors. About 1 σ of this difference is due to the larger secondary production we use.

Sulpher. For ^{34}S our source abundance fraction is ~ 1 σ lower than that reported by Wiedenbeck, 1984. In arriving at a source abundance we use a secondary production ~ 33% larger than that which appears to have been used by Wiedenbeck. The actual cosmic ray source abundance ratios we find for both ^{33}S and ^{34}S are consistent with zero. This is not a realistic value, however, since the interstellar secondary production is ~ 5 x the source abundance ratio for ^{34}S and the experimental errors in all measurements to date are greater than the source abundance fraction itself.

Argon & Calcium. Both of these charges are somewhat different than the previous charges discussed. Individually they are dominated by one rather rare isotope in the source, ^{36}Ar or ^{40}Ca and the possible source abundances of the other isotopes are expected to be completely dominated by interstellar secondary production if we consider solar system abundance fractions. The isotopic abundance fractions that we measure as shown in Table I are indeed consistent with purely secondary production with the exception of ^{36}Ar and ^{40}Ca. The fractions of these isotopes we measure are ~ 1.5 x larger than expected for pure solar system abundances however. This could be suggestive of a somewhat larger abundance of these isotopes relative to Fe in the cosmic ray source. Unfortunately we are unable to derive absolute ratios of these isotopes to Fe from this analysis to confirm this suggestion.

3. Summary. In this analysis we find one decisive example of an isotopic abundance difference in the cosmic ray source, ^{22}Ne as has been observed several times before. We also find a suggestion that ^{25}Mg & ^{26}Mg are enhanced but only at the 1 σ level. For

all of the other isotopes we measure, including ^{29}Si & ^{30}Si, our results are consistent with a solar system isotopic composition. About 30% of the difference in the source abundance ratio derived in this paper and those previously reported appears to be due to differences in the cross sections used, the remaining differences are in the experimental results themselves.

4. Acknowledgements. This work was supported by NASA grant NGR - 30-002-052.

5. References.

Wiedenbeck, M. E., & Greiner, D. E., Phys. Rev., 48, 682, 1981a
Wiedenbeck, M. E., & Greiner, D. E., Ap. J., 247, L122, 1981b
Wiedenbeck, M. E., Proc. 18th ICRC, 9, 147, 1983
Wiedenbeck, M. E., paper presented at COSPAR symposium, Graz., August, 1984

6. Figure Captions.

Figure 1. C x E matrix of events for Oxygen nuclei. Calculated mass lines for ^{15}O, ^{16}O, ^{17}O and ^{18}O are shown.
Figure 2. Mass histograms for N, O, Ne and Mg nuclei.
Figure 3. Mass histograms for Al, Si, S, Ar and Ca nuclei

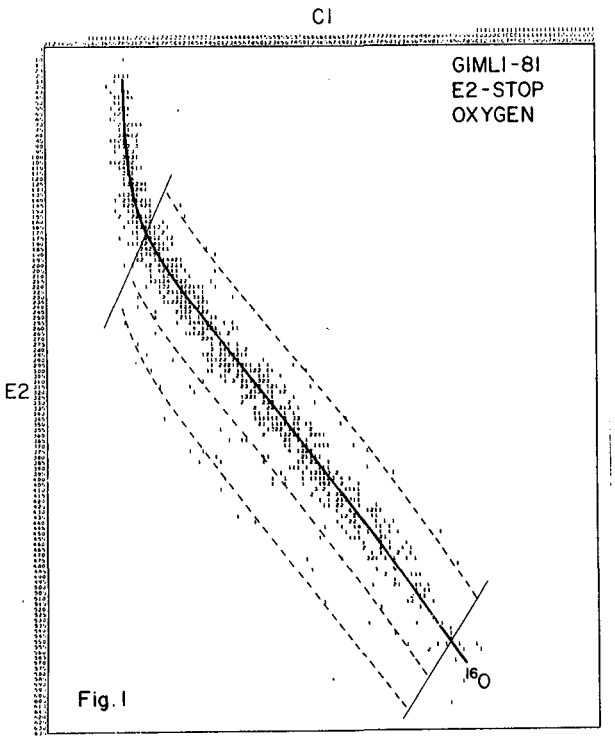

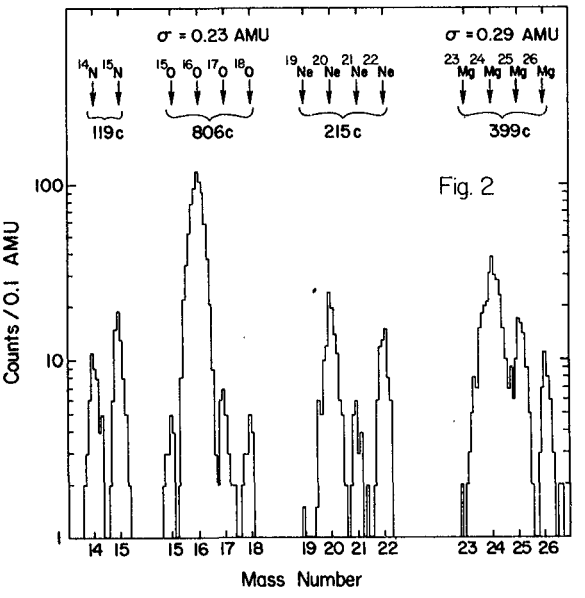

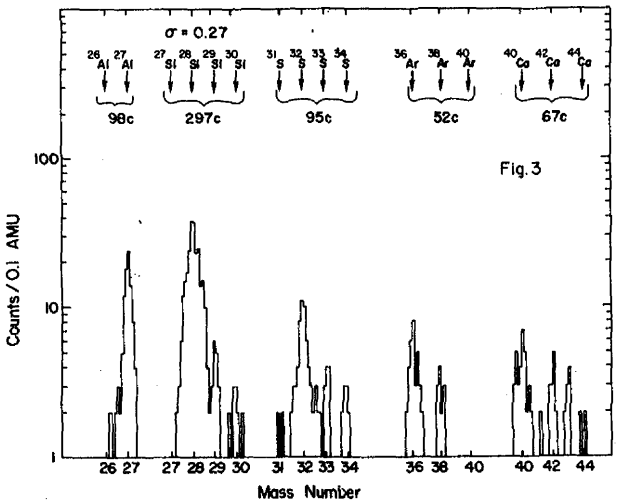

Table I

Isotopic Abundances

Isotope	Energy Interval (MeV/nuc)	Events Observed	% of Charge equal E int.	% of Charge at Top of Atm	Predicted*
^{14}N	383 - 450	49	39.7	38.2±5.6	
^{15}N	375 - 438	70	60.3	61.8±5.1	
^{16}O	390 - 485	752	94.1	94.4	
^{17}O	386 - 472	22	3.0	2.8±0.6	
^{18}O	381 - 460	19	2.8	2.7±0.6	
^{20}Ne	410 - 554	121	55.0	54.7	
^{21}Ne	406 - 542	23	11.0	10.6±2.1	
^{22}Ne	401 - 530	67	34.0	34.7±4.0	
^{24}Mg	429 - 610	270	66.5	64.8	
^{25}Mg	425 - 601	66±8	17.0	17.5±2.6	
^{26}Mg	420 - 592	61	16.5	17.7±2.4	
^{26}Al	435 - 635	5±3	5.0	2.2±1.8	
^{27}Al	430 - 627	94	95.0	97.8	
^{28}Si	446 - 642	251	88.1	88.7	
^{29}Si	441 - 637	18±3	6.3	5.9±1.8	
^{30}Si	436 - 632	16	5.6	5.4±1.5	
^{32}S	462 - 660	64	68.7	69.9	
^{33}S	457 - 656	14	15.2	14.5±3.9	
^{34}S	453 - 651	15	16.1	15.6±4.1	
^{36}Ar	478 - 678	33	63.5	63.7	42.6
^{37}Ar	474 - 674	2	3.8	2.6±2.0	12.8
^{38}Ar	470 - 669	16	30.8	31.4±8.7	38.9
^{39}Ar	466 - 665	0	0.0	0.0	0.0
^{40}Ar	462 - 660	1	1.9	2.2±2.2	5.7
^{40}Ca	494 - 697	31	46.1	46.9	30.8
^{41}Ca	490 - 692	~3	4.5	4.1±2.7	6.2
^{42}Ca	486 - 688	16	24.0	23.8±6.6	22.0
^{43}Ca	482 - 684	10	15.0	14.3±5.1	19.8
^{44}Ca	478 - 680	7	10.4	10.9±4.4	21.2

* Assuming $\left(\frac{^{36}Ar}{Fe}\right)_S = 3.0\%$, $\left(\frac{^{40}Ca}{Fe}\right)_S = 6.8\%$

TABLE II

Isotope Fractions

Ratio	This Measurement (%)	Wiedenbeck, 1984 (%)	Secondary Production (%)	Cosmic Ray Source (%)	Solar System (%)
$^{17}O/^{16}O$	2.9±0.7	1.7±0.4	2.1	0.8±0.6	-
$^{18}O/^{16}O$	2.8±0.7	1.9±0.2	2.1	0.7±0.6	0.2
$^{21}Ne/^{20}Ne$	19.4±4.1	21±5	20.5	-1.1±4.5	0.3
$^{22}Ne/^{20}Ne$	63.4±8.6	58±6	16.5	46.9±9.0	12.2
$^{25}Mg/^{24}Mg$	27.1±4.4	27±4	8.6	18.5±4.6	12.9
$^{26}Mg/^{24}Mg$	27.4±2.6	27±3	10.1	17.3±4.0	14.2
$^{29}Si/^{28}Si$	6.9±2.0	13±2	3.3	3.6±2.7	5.1
$^{30}Si/^{28}Si$	6.4±1.8	7.2±1.7	3.8	2.6±2.3	3.4
$^{33}S/^{32}S$	20.7±5.8	-	20.5	0.2±6.4	0.8
$^{34}S/^{32}S$	22.5±6.1	28±8	23.2	-0.7±6.7	4.4